Journal of Marine Research, 63, 863–885, 2005

Journal of
MARINE RESEARCH

Volume 63, Number 5

On the subduction of upwelled waters in the California Current

by Steven J. Bograd[1] and Arnold W. Mantyla[2]

ABSTRACT

We use 20 years of hydrographic data from the California Cooperative Oceanic Fisheries Investigations (CalCOFI) program off southern California to search for water mass signatures of subducted upwelled waters. A search for secondary oxygen maxima in more than 6000 water column profiles identified 629 cases of deep oxygen inversions. The additional criteria of a minimum magnitude of the deep oxygen inversion and an accompanying reduction in dissolved nutrients identified 106 (~17%) of these as subduction signatures. The physical and chemical characteristics of these water masses suggest that they had been photosynthetically modified in the euphotic zone, and perhaps ventilated at the surface, before being subducted and eventually advected downstream within the California Current. Surface waters with similar physical characteristics as the subduction signatures (θ~8.5°C, S~34.0 psu, σ_θ~26.4 kg m^{-3}) were observed during the spring-summer upwelling period at a shore station upstream from the CalCOFI grid. Even with conservative search criteria and coarse spatial-temporal sampling, subduction signatures were observed in all seasons and in each year of the record. These results imply that the processes leading to the subduction, cross-shore transport, and downstream advection of upwelled water masses are common and persistent in the California Current. This has important implications for the transport of coastal waters, and resident planktonic organisms and organic carbon, out of the coastal euphotic zone, and provides a mechanism for frequent ventilation of the upper thermocline of the California Current.

1. Introduction

Strong coastal upwelling supports a productive ecosystem in the California Current System (CCS) (Wooster and Reid, 1963). The seasonally varying wind forcing also drives

1. NOAA, Pacific Fisheries Environmental Laboratory, Pacific Grove, California, 93950-2097, U.S.A. ***email: steven.bograd@noaa.gov***
2. Scripps Institution of Oceanography, La Jolla, California, 92093-0224, U.S.A.

a strong annual cycle in the dynamics of the CCS (Hickey, 1979; Lynn and Simpson, 1987; Lynn *et al*., 2003). A strong coastal equatorward jet develops with the onset of upwelling each spring, independent of the winter manifestation of the offshore California Current core (Strub and James, 2000; Lynn *et al*., 2003). Baroclinic processes lead to the development of nearshore filaments and mesoscale eddies which propagate offshore and result in a maximum in offshore eddy kinetic energy in summer-fall (Chereskin *et al*., 2000; Strub and James, 2000). These mesoscale features are important cross-shore transporters of coastal waters and the biogenic material contained therein. Furthermore, the internal dynamics associated with these features could result in the subduction of water masses out of the coastal euphotic zone. In particular, upwelling-induced cold filaments have been shown to subduct coastal water masses and transport them offshore (Flament *et al*., 1985; Kadko *et al*., 1991; Washburn *et al*., 1991; Barth *et al*., 2002). It is important to quantify these processes in order to better understand the ultimate fate of coastally upwelled waters.

A secondary oxygen maximum occasionally appears in the upper thermocline of the California Current off southern California. The source of this signal is unknown, but could arise from biological cycles and surface gas exchange within upwelled waters upstream (Stefansson and Richards, 1964). A newly upwelled water mass would stimulate phytoplankton production, resulting in consumption of inorganic nutrients newly imported into the euphotic zone, decay of organic matter, and respiration. Such a water mass would have discernable physical properties typical of waters found at depths along the continental shelf, as well as photosynthetically modified chemical signatures, i.e., excess oxygen and reduced nutrients. If subducted, these water masses could retain their chemical and biological properties for some time as they are advected within the equatorward flow of the California Current.

In this manuscript, we explore 20 years of hydrographic data collected within the southern CCS under the auspices of the California Cooperative Oceanic Fisheries Investigations (CalCOFI). Our objectives are to search for the downstream signatures of subducted water masses in the CalCOFI record, and to (a) determine the frequency of occurrence of these features, (b) quantify their spatial and temporal distribution, and (c) describe their physical and chemical properties. This census of subducted water masses will contribute to assessing the importance of the subduction process in transporting coastal, biologically active water masses offshore, and will lead to a better understanding of the evolution and fate of coastally upwelled waters.

2. Data and methodology

a. CalCOFI hydrographic data

The current CalCOFI sampling grid extends from the U.S.-Mexico border to just north of Pt. Conception and out to several hundred kilometers offshore, with six nominal lines oriented approximately perpendicular to the coastline (Fig. 1). There are nearly 70 stations occupied regularly within this grid, designated by a line and station number (e.g., 77.60 is

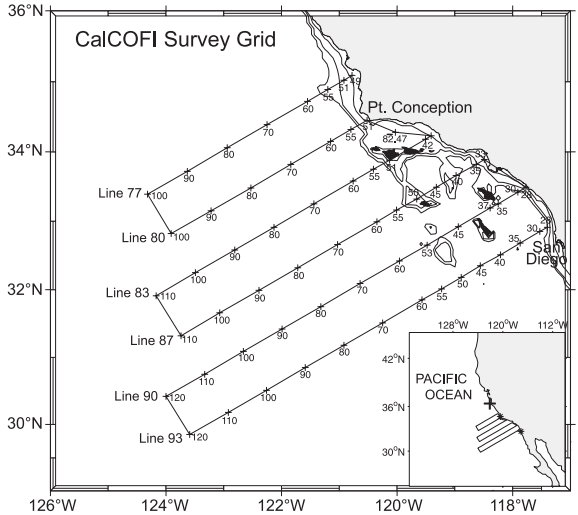

Figure 1. Map of the region showing the modern CalCOFI sampling grid, occupied quarterly. The 100, 300, and 500-m isobaths are shown. The '+' in the inset marks the location of the Granite Canyon shore station.

station 60 on line 77). Nominal station spacing is approximately 70 km offshore, but considerably less inshore of station 60. The current grid has been occupied at least quarterly since 1984, with target months of January, April, July, and October. More than 6000 station occupations have been made on this grid between January 1984 and January 2004. Although CalCOFI has sampled portions of the California Current since 1949, we have confined our analysis to the post-1984 (January 1984 – January 2004) data set, when a standard set of stations was occupied quarterly and concomitant measurements of dissolved oxygen and inorganic nutrients were made. Non-CalCOFI data obtained from the same region over the post-1984 period has been excluded from the analysis.

Routine CalCOFI station occupations since April 1993 have deployed a SeaBird CTD instrument with a 24-place rosette, which is equipped with 24 10-L plastic (PVC) Niskin bottles (Scripps Institution of Oceanography, 2002). (Epoxy-coated Nansen wire casts were done prior to August 1987; 3-L PVC bottle wire casts were done from September 1987 through April 1993.) Casts were made to ~525-m depth, bottom depth permitting. Bottle samples were generally chosen to provide good resolution ($<$10 m) around the chlorophyll, oxygen, and nitrite maxima and the shallow salinity minimum of the upper thermocline. Pressures and temperatures for each water sample were derived from the CTD signals recorded just prior to the bottle trip. Salinities were analyzed at sea from the bottle data using a Guildline model 8410 Portasal salinometer, with the results compared to the CTD salinities to check for mistrips or leaks (Scripps Institution of Oceanography, 2002). Dissolved oxygen samples were collected in calibrated 100 mL iodine flasks and analyzed at sea by the modified Winkler method (Carpenter, 1965), using the equipment and procedure outlined by Anderson (1971). Percent oxygen saturation was calculated from the

equations of Garcia and Gordon (1992). Dissolved silicate, phosphate, nitrate and nitrite concentrations were determined at sea using an automated analyzer (Atlas *et al*., 1971), following procedures similar to those described in Gordon *et al*. (1993). Estimates of precision of these standard techniques are 0.01°C, 0.002 psu, 0.02 mL L^{-1} for dissolved oxygen, and 0.5, 0.01, and 0.1 μMol L^{-1} for silicate, phosphate, and nitrate, respectively (Scripps Institution of Oceanography, 1991). Samples for chlorophyll-*a* and phaeopigments were collected in calibrated 138 mL polyethylene bottles and filtered onto Whatman GF/F filters. These samples were taken only in the upper 200 m, generally above any secondary oxygen maxima. Further details of the standard sampling and analysis procedures, along with all data and derived variables, can be found in any of the CalCOFI data report series (e.g., Scripps Institution of Oceanography, 2002).

b. Shore station time series

Time series of surface temperature and salinity are available from a number of shore stations along the U.S. west coast (available from Scripps Institution of Oceanography at http:// www-mlrg.ucsd.edu/shoresta/index.html). We present data from the Granite Canyon, California station (36°25.9'N, 121°55'W; see Fig. 1), which is representative of the seasonal upwelling domain of the central California coast. Daily temperature measurements were made with a Kahl Scientific stem mercury immersion thermometer which is regularly calibrated and has an accuracy of 0.01°C. Daily water samples are run on a Guildline 8410 salinometer, providing salinity values to two decimal places. The Granite Canyon temperature series extends from 1971–2000, while the salinity series extends from 1986–2000. Both records contain numerous data gaps of varying length that have not been filled. These data are used to identify the source waters for the subduction signatures identified downstream in the CalCOFI region.

c. Search for subducted water masses

Our objective is to identify water masses observed in the CalCOFI historical record that have undergone a specific history: upwelled from depth near the coast upstream, modified through photosynthetic activity, subducted to a neutral density, and advected within the equatorward flow of the California Current into the CalCOFI domain. We expect that such water masses would have the characteristic signature of a deep oxygen maximum accompanied by a reduction in dissolved nutrients. The relatively high oxygen could result from surface ventilation as well as photosynthesis, while the nutrient reduction would be indicative of utilization by phytoplankton. These waters would not necessarily have reached the surface, so there would not likely be significant changes in the temperature or salinity and thus no defining T-S signature associated with this water mass. However, the T-S properties would be representative of waters that are brought up from depth near the coast, rather than waters of subarctic origin that typically compose the California Current. Based on these expectations, the search for such water masses involved an examination of all (6000+) station profiles from the CalCOFI grid over the 20-year period January 1984 to January 2004, with the aim of identifying deep inversions in the oxygen and nutrient

profiles. The 70-km grid spacing over much of the CalCOFI survey grid generally precludes resolution of the dynamics associated with these features.

Because a shallow oxygen maximum is a persistent feature of California Current waters (Reid, 1962; Hayward, 1994), it was necessary to confine the search for oxygen inversions to depths below this feature. A preliminary search identified all oxygen inversions (increases from one bottle to the next deepest greater than 0.1 mL L^{-1}) below 150 m, which is an arbitrary depth but one that is consistently below the shallow oxygen maximum throughout the CalCOFI region. The 0.1 mL L^{-1} cutoff for the oxygen increase is a conservative criterion that eliminates the identification of potentially erroneous oxygen measurements. This search identified more than 600 events (typically a single bottle in a profile) in the CalCOFI record, at a mean potential density of approximately $\sigma_\theta = 26.4 \pm 0.1$. This search may have missed candidate events at a shallower level, particularly closer to the coast where the isopycnals slope strongly upward. The search for deep oxygen inversions was repeated using the criterion of all depths greater than two standard deviations below the mean potential density of the events identified in the preliminary search (i.e., $\sigma_\theta \geq 26.13$). This search identified 629 *deep oxygen inversions* that met the criteria described above. Although these features may represent subducted water masses, we use the following additional criteria on the subset of identified deep oxygen inversions: (a) a minimum magnitude of the oxygen inversion (an increase equivalent to at least 0.1 mL L^{-1} over a depth of 10 m) and (b) an accompanying nitrate reduction (a decrease in nitrate from one bottle to the next deepest that accompanies the strong oxygen inversion). A total of 106 features, which we call *subduction signatures*, met these additional criteria. The physical and chemical characteristics of the 629 deep oxygen inversions and 106 subduction signatures are described in the following section.

Although evaluation of hydrographic data can be a subjective process, internal checks were used to determine if the identified oxygen anomalies were real: (1) an unprotected (pressure-sensitive) thermometer verifies that the sampling bottle tripped at the intended depth; (2) the combined temperature and salinity information results in a smooth and stable density profile, verifying that the sampling bottle did not leak; and (3) a concomitant nutrient inflection strongly implies that the oxygen anomaly is not due to analytical error. It is not likely that any other set of processes other than the subduction and subsequent advection of upwelled, biologically modified waters would result in water masses meeting these criteria and having the characteristics described above.

3. Results

a. A case study: August 1985

A representative example of a strong subduction signature was the one observed on the CalCOFI cruise of August 9–22, 1985. Water column profiles of temperature, salinity, oxygen, oxygen saturation, nitrate, and phosphate at station 80.80 (33°28.8'N, 122°31.8'W) clearly show a strong secondary oxygen (3.98 mL L^{-1}) and saturation (60.1%) maximum centered at $\sigma_\theta = 26.45$ (depth of 214 m) which is accompanied by reductions in dissolved

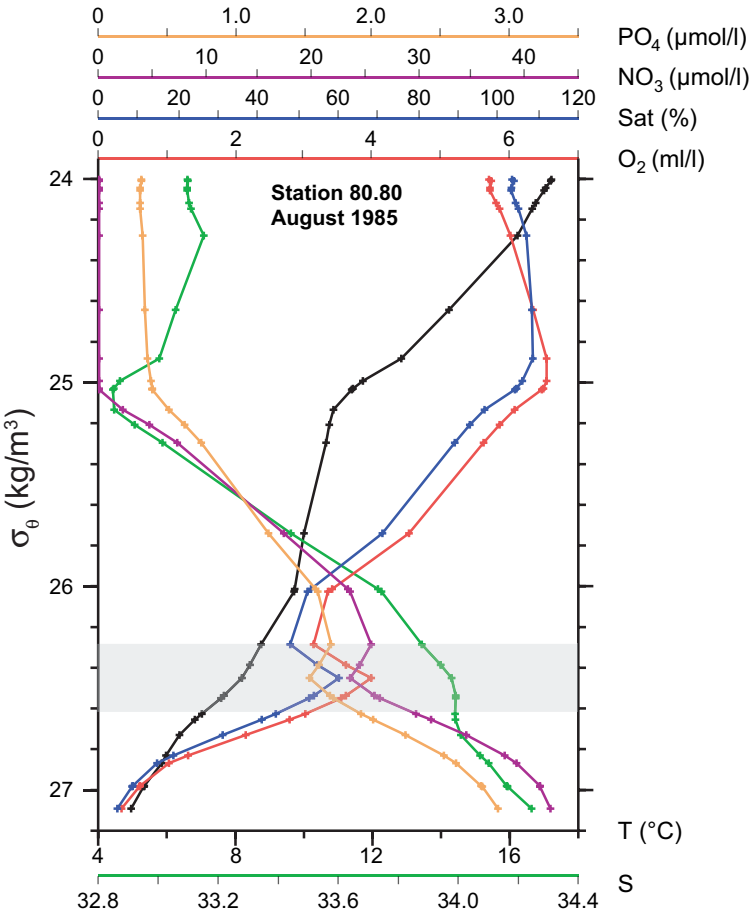

Figure 2. Profiles of temperature (black), salinity (green), dissolved oxygen (red), oxygen saturation (blue), nitrate (purple), and phosphate (orange) for station 80.80 in August 1985. The layer containing the subduction event is marked by the translucent box.

nitrate and phosphate (Fig. 2). This feature was well below the shallow oxygen maximum, which peaked at 6.54 mL L^{-1} (108.6% saturation) at σ_θ = 24.99 (64 m), and was just below a shallow oxygen minimum of 3.14 mL L^{-1} at σ_θ = 26.29 (183 m). A similar feature was observed at approximately the same density level on profiles for the adjoining stations 80.70, 77.80, and 77.90, encompassing an area of at least 40 x 40 square nautical miles. A comparison of surrounding station profiles indicated that the deep oxygen maximum was the anomalous feature, rather than the shallow oxygen minimum overlaying it. The magnitude of the deep inversions at station 80.80 was 0.84 mL L^{-1}, −2.0 µMol L^{-1}, and −0.18 µMol L^{-1} over a depth of 31 m for oxygen, nitrate, and phosphate, respectively. The reduced nutrients at the same depth as the excess oxygen imply the feature is of photosynthetic origin and was recently at a shallower level. The temperature and salinity

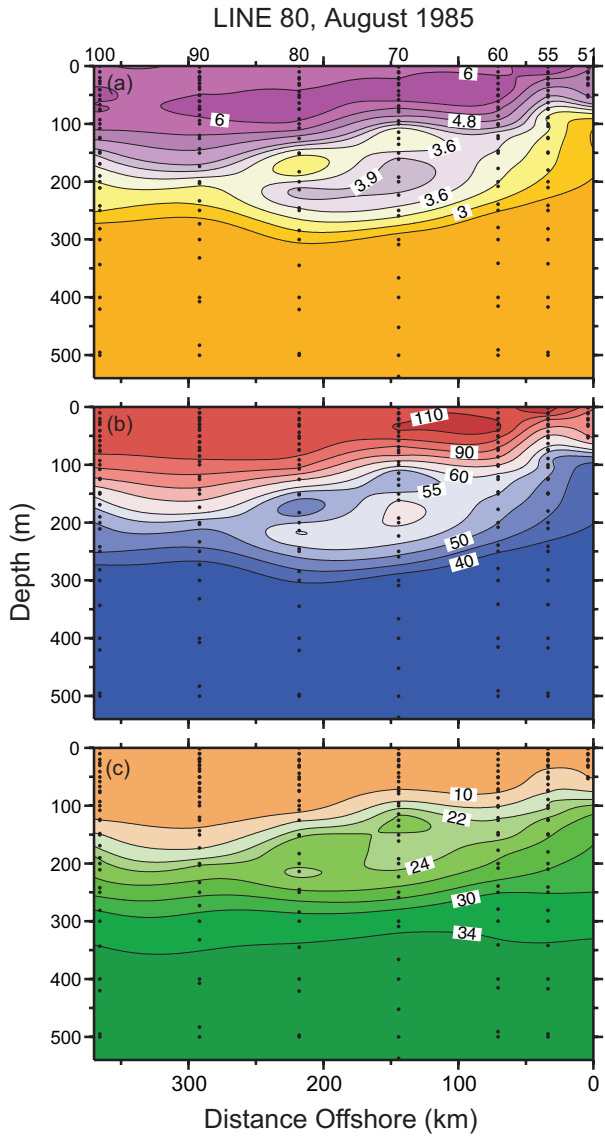

Figure 3. Sections of (a) dissolved oxygen (mL L^{-1}), (b) oxygen saturation (%), and (c) nitrate (μMol L^{-1}) for line 80 in August 1985. The stations are labeled on the top axis in (a), and all bottle locations are marked.

on the $\sigma_\theta = 26.45$ surface at station 80.80 was 8.17°C and 33.98 psu, similar to the water properties seen within the upper 50 m on the shelf off Pt. Reyes (37.9N) in April and May, 1984 (stations 60.50 and 60.55; Scripps Institution of Oceanography, 1984).

Oxygen, oxygen saturation, and nitrate sections on line 80 show the spatial extent of the feature in the cross-shore and vertical directions (Fig. 3). The feature is evident from

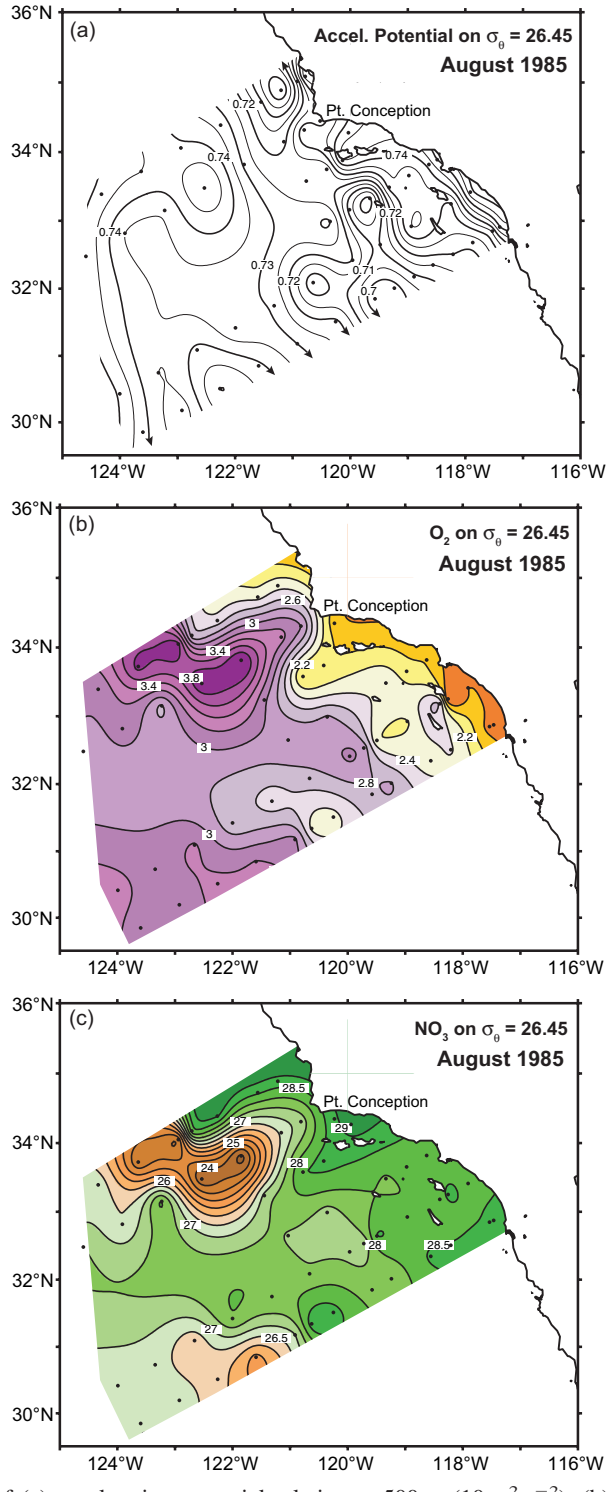

Figure 4. Maps of (a) acceleration potential relative to 500 m (10 $m^2\ s^{-2}$), (b) dissolved oxygen (mL L^{-1}), and (c) nitrate (μMol L^{-1}) on the σ_θ = 26.45 density surface in August 1985. All station locations are marked. Some of the nominal offshore stations on lines 83 and 87 were not occupied on this cruise.

several bottle samples at stations 80.80 and 80.70 (a width of at least 70 km) and encompasses a layer approximately 100 m (0.3 σ_θ) thick. Isopycnal maps of oxygen and nitrate further delineate the dimensions of this feature (Fig. 4). Comparably high (low) oxygen (nitrate) values were observed at this density level at the adjoining stations 80.70, 80.80, 77.80, and 77.90. The acceleration potential on the $\sigma_\theta = 26.45$ surface shows a generally equatorward flow over most of the grid and poleward flow at the coast (Fig. 4a). The anomalous chemical properties evident on lines 77 and 80 are contained within an anticyclonic eddy that is embedded in the equatorward flow of the California Current.

The $\sigma_\theta = 26.45$ surface was observed shallower than 100 m on CalCOFI cruises 8404 and 8405 along the California coast between San Francisco and Monterey (Scripps Institution of Oceanography, 1984; later cruises only sampled from near Pt. Conception southward; see Fig. 1). Surface temperatures at the Granite Canyon shore station were less than 9°C in the spring of 1984 and 1985 (not shown), and coastal surface temperatures of less than 9°C are often observed near Cape Mendocino (40.5N). We also note that the eddy seen in Figure 4a was evident at the 200 m (200/500 dbar) dynamic height field, but was not evident in the surface (0/500 dbar) dynamic height field, which showed the core of the California Current entering the survey grid from the northwest between stations 77.80 and 77.90 and a strong equatorward flow through the middle of the grid (Scripps Institution of Oceanography, 1986). The implication is that the anomalous feature centered near $\sigma_\theta = 26.45$, which has characteristic signatures of biologically modified upwelled waters, was advected by the main California Current into the CalCOFI region within a coherent mesoscale feature that may have limited mixing with surrounding waters.

b. Census of deep oxygen inversions and subduction signatures

Applying the search criteria described in Section 2c to all data over the period January 1984 to January 2004 identified numerous deep oxygen inversions and subduction signatures throughout the record. Deep oxygen inversions were observed in all seasons and all years, with a higher proportion in summer than the other seasons (Table 1). There were 28% (41%) more deep oxygen inversions observed in summer than in winter (spring), even though the distribution of total station occupations was nearly the same in each season. Frequency distributions of the magnitude and density level of the deep oxygen inversions, however, show little seasonal variation (Fig. 5). The oxygen inversions are strongest in summer, but not significantly so. The densities of the inversions are nearly normally distributed, with the densest events ($\sigma_\theta > 26.9$) observed at stations 77.80 in January 2004 and 80.70 in October 2003. Overall, the physical and chemical properties of the deep oxygen inversions, and their location within the water column, are very similar in each season (Table 1). A majority of these features (>80%) do not have a corresponding nutrient reduction, that is the nitrate profile shows a steady increase with depth, as is normally observed, through the observed oxygen inversion.

The mean temperature-salinity characteristics of the deep oxygen inversions (~8.4°C, 34.00 psu) are characteristic of the source waters for coastal upwelling, rather than the considerably less saline waters of either offshore or subarctic origin that compose typical

Table 1. Seasonal statistics of all identified deep oxygen inversions in the CalCOFI record, January 1984 to January 2004. See Section 2c for event identification details. Property mean and one standard deviation are shown. Units on the oxygen gradient are (mL L^{-1} m^{-1} × 1000). Units on the nitrate gradient are (μMol L^{-1} m^{-1} × 1000). The number of features in each season is given in parentheses. Winter is January–March, spring is April–June, summer is July–September, and autumn is October–December.

	Winter (152)	Spring (124)	Summer (211)	Autumn (142)
P (dbar)	215.5 ± 52.0	214.7 ± 45.7	220.6 ± 63.6	229.5 ± 57.3
θ (°C)	8.41 ± 0.69	8.28 ± 0.55	8.28 ± 0.67	8.26 ± 0.69
S (psu)	33.98 ± 0.09	33.97 ± 0.09	34.02 ± 0.11	34.00 ± 0.09
σ_θ (kg m^{-3})	26.41 ± 0.14	26.43 ± 0.13	26.46 ± 0.14	26.46 ± 0.14
O_2 (mL L^{-1})	2.99 ± 0.67	3.08 ± 0.63	2.73 ± 0.80	2.85 ± 0.75
O_2 sat. (%)	45.4 ± 10.3	46.7 ± 9.8	41.4 ± 12.1	43.2 ± 11.5
NO_3 (μMol L^{-1})	26.55 ± 3.14	26.49 ± 3.15	27.67 ± 3.36	27.48 ± 3.50
O_2 gradient	9.4 ± 6.7	9.4 ± 7.0	9.7 ± 6.8	9.4 ± 7.1
NO_3 gradient	18.4 ± 34.3	17.7 ± 30.0	14.7 ± 31.7	17.1 ± 30.5

California Current waters (~33.0–33.4 psu; Lynn and Simpson, 1987). Undoubtedly, many of these deep oxygen inversions represent water masses that have undergone the upwelling and subduction history we are looking for. However, the definitive signature of a subducted coastal water mass includes a deep oxygen inversion accompanied by a

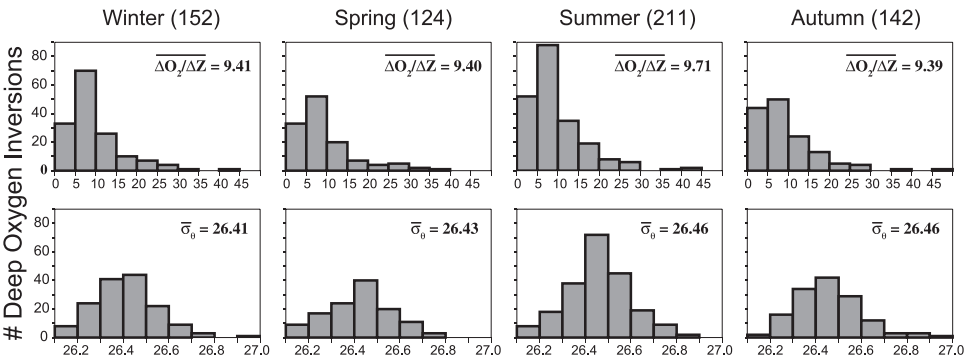

Figure 5. Seasonal frequency distribution of the magnitude of the oxygen inversion (top panels) and density level (bottom panels) for all identified deep oxygen inversions in the CalCOFI record, January 1984 to January 2004. See Section 2c for event identification details. For each seasonal subset, total number of identified features is labeled above top panels and mean property values are labeled within panels. Units on the oxygen inversion are (mL L^{-1} m^{-1} × 1000). Winter is January-March, spring is April-June, summer is July-September, and autumn is October-December.

Table 2. Seasonal statistics of all identified subduction signatures in the CalCOFI record, January 1984 to January 2004. See Section 2c for event identification details. Property mean and one standard deviation are shown. Units on the oxygen gradient are (mL L^{-1} m^{-1} × 1000). Units on the nitrate gradient are (μMol L^{-1} m^{-1} × 1000). The number of features in each season is given in parentheses. Seasons defined as in Table 1.

	Winter (24)	Spring (24)	Summer (37)	Autumn (21)
P (dbar)	210.9 ± 33.7	201.3 ± 35.3	204.1 ± 33.7	216.5 ± 28.6
θ (°C)	8.36 ± 0.37	8.46 ± 0.38	8.30 ± 0.40	8.25 ± 0.49
S (psu)	33.95 ± 0.05	33.94 ± 0.06	33.97 ± 0.07	33.96 ± 0.03
σ_θ (kg m^{-3})	26.39 ± 0.07	26.37 ± 0.09	26.42 ± 0.08	26.42 ± 0.09
O_2 (mL L^{-1})	3.69 ± 0.49	3.51 ± 0.33	3.38 ± 0.59	3.50 ± 0.44
O_2 sat. (%)	55.9 ± 7.5	53.4 ± 5.2	51.2 ± 9.1	53.0 ± 7.1
NO_3 (μMol L^{-1})	24.01 ± 2.29	24.52 ± 1.76	25.39 ± 2.45	24.95 ± 2.61
O_2 gradient	20.3 ± 8.2	20.0 ± 7.8	19.4 ± 7.7	17.0 ± 7.3
NO_3 gradient	−39.8 ± 31.3	−27.0 ± 26.5	−31.5 ± 34.5	−31.8 ± 27.1

reduction in nutrients (see Section 2c). Only 106 of the deep oxygen inversions (~17%) met these criteria and are classified as subduction signatures. The properties of these features are remarkably similar to the deep oxygen inversions (Table 2). Their T-S characteristics (~8.3°C, 33.95 psu) are again indicative of water masses of coastal upwelling origin. The oxygen (and saturation) anomalies are considerably larger than those of the deep oxygen inversions, but this is partly because a minimum oxygen gradient was one of the identifying criteria. Note that the mean nitrate changes associated with the oxygen inversions are always negative (again as a requirement of the identifying criteria), and amount on average to a reduction of approximately 1.0 μMol L^{-1} over a vertical depth of 33 m (Table 2). The mean oxygen inversion was approximately 0.66 (1.0) mL L^{-1} over the same vertical distance (50 m).

Frequency distributions of the density level, potential temperature, and salinity of the subduction signatures show some seasonal variation (Fig. 6). There were 35–40% more subduction signatures observed during summer compared to the rest of the year. As with the deep oxygen inversions, a nearly equivalent number of subduction signatures were observed in autumn, winter, and spring. Subduction signatures were observed at densities greater than $\sigma_\theta = 26.5$ only in summer and autumn (Fig. 6), and at slightly greater depths in autumn (Table 2). These unusually deep features were due to cooler water masses in autumn, and to either cooler or saltier water masses in summer. The mean density levels, however, remained remarkably consistent throughout the year, with very little intraseasonal variation (standard deviations of ~0.08 σ_θ). The mean chemical properties and

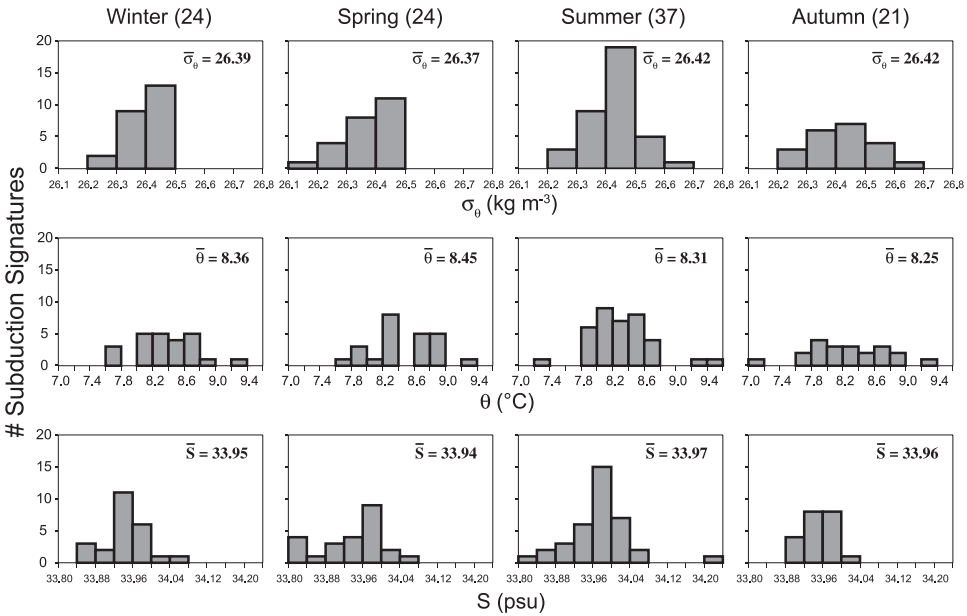

Figure 6. Seasonal frequency distribution of the density level (top panels), potential temperature (middle panels), and salinity (bottom panels) for all identified subduction signatures in the CalCOFI record, January 1984 to January 2004. See Section 2c for event identification details. For each seasonal subset, total number of identified features is labeled above top panels and mean property values are labeled within panels. Seasons defined as in Figure 5.

magnitude of oxygen and nutrient anomalies of the subduction signatures were not significantly different between seasons (Table 2).

There appears to be a strong relationship between the magnitudes of the oxygen inversion and nitrate reduction for the subduction signatures ($r = -0.78$; Fig. 7). The implication is that the processes that form the oxygen and nutrient anomalies (magnitude, duration, and source waters of upwelling, potential for ventilation, photosynthesis and nutrient uptake by phytoplankton, and respiration) are linked, as we have hypothesized. The degree of water mass modification may depend more on the persistence of an upwelling event rather than its strength. Since upwelling event-lengths vary greatly, there will be varying degrees of exposure to sunlight and photosynthesis. A majority of subduction signatures had oxygen inversions and nitrate reductions less than 0.6 mL L^{-1} and 1.5 μMol L^{-1}, respectively, over a vertical distance of 30 m. However, there were 10 features, from all seasons, with oxygen inversions greater than 0.9 mL L^{-1} over 30 m, and 5 features with nitrate reductions greater than 3 μMol L^{-1} over 30 m. No relationship was found between the magnitude of the oxygen inversion and its density level, nor between the density level and the latitude of the observed subduction signatures. Nor were there any significant relationships between the observed properties of the deep oxygen inversions (not shown).

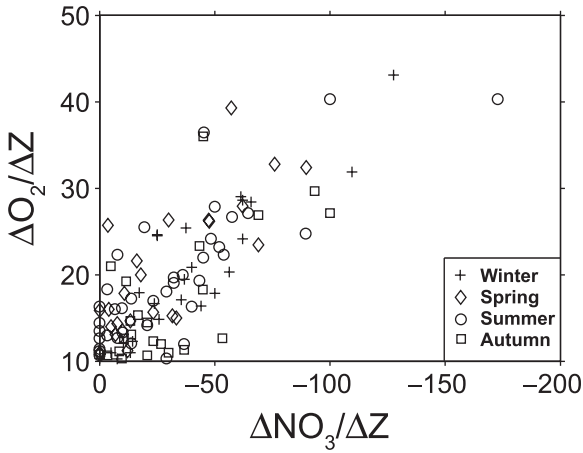

Figure 7. Scatter plot of magnitude of oxygen inversion (mL L^{-1} m^{-1} × 1000) vs. magnitude of nitrate reduction (μMol L^{-1} m^{-1} × 1000) for all identified subduction signatures in the CalCOFI record, January 1984 to January 2004. Seasons defined as in Figure 5.

The higher number of observed subduction signatures in summer (35% of total; Table 2) suggests that these features may have been recently formed during that year's upwelling season, which typically peaks in May–June off central and northern California. However, the temporal distribution of the subduction signatures will depend on the lag time between the formation and subsequent observation of the water mass downstream, which could be substantial, as well as on the formation location. Peak upwelling progresses to later in the year as one proceeds northward from Baja to Oregon (Reid *et al.*, 1958). The fact that subduction signatures were observed year-round suggests that (a) the necessary formation processes may occur throughout the year along some portions of the coast and/or (b) these water masses, once formed and subducted, can be long-lived, with autumn and winter features possibly having originated during the previous upwelling season.

The frequency of occurrence of subduction signatures in the CalCOFI region presents a pattern that clearly delineates the seasonal evolution of the California Current (Fig. 8). Most stations on the CalCOFI grid had fewer than 2% of occupations with an observed subduction signature in any season. But the stations composing the central portion of the grid, which represent the mean breadth of the core of the California Current, had the highest frequency of occurrences in each season. This path of high occurrences is especially evident in spring and summer and is located farther offshore in autumn and winter, mirroring the seasonal offshore migration of the California Current core (Lynn and Simpson, 1987; Lynn *et al.*, 2003). By contrast, the coastal stations near Pt. Conception, which is the area with strongest seasonal upwelling in southern California, had very low (or no) occurrences of subduction signatures throughout the year. These patterns again imply that the anomalous water masses are formed upstream and advected into the region within the main flow of the California Current. The highest frequency of occurrences, ∼17% of

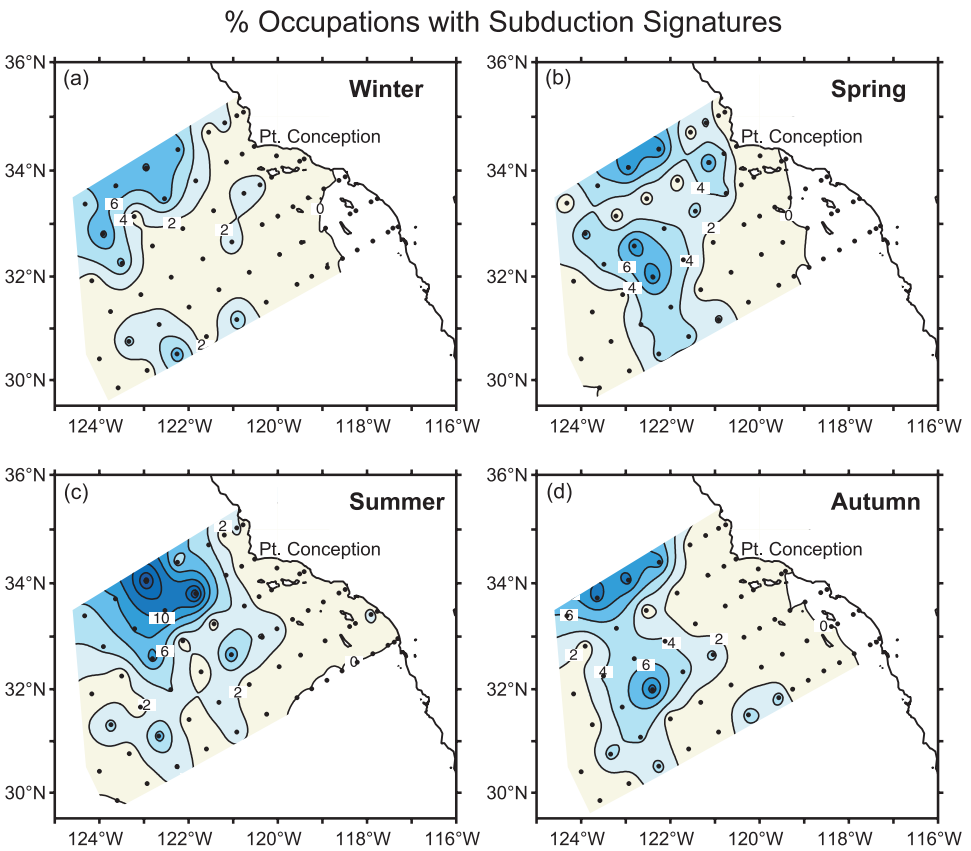

Figure 8. Seasonal maps of percent of total number of occupations in which a subduction signature has been identified in the CalCOFI record, January 1984 to January 2004. All station locations are marked. Seasons defined as in Figure 5.

summer occupations, were at stations 77.80 (4 of 23 occupations) and 80.70 (5 of 30), which is typically where the California Current enters the grid from the northwest (Fig. 8c).

4. Discussion

a. The source waters

If the age of the subduction signatures could be determined, we would be able to identify the time and presumed location at which the water mass was formed. However, we are likely observing water masses of various ages and from different sources (latitude and depth) along the U.S. west coast, which have undergone some degree of mixing with *in situ* waters during their path to southern California. Thus, the magnitude of the oxygen and nutrient anomalies will not necessarily imply the age or degree of photosynthetic modification of the water mass following an upwelling event. But we can determine whether waters having the physical characteristics seen in Tables 1 and 2 are observed

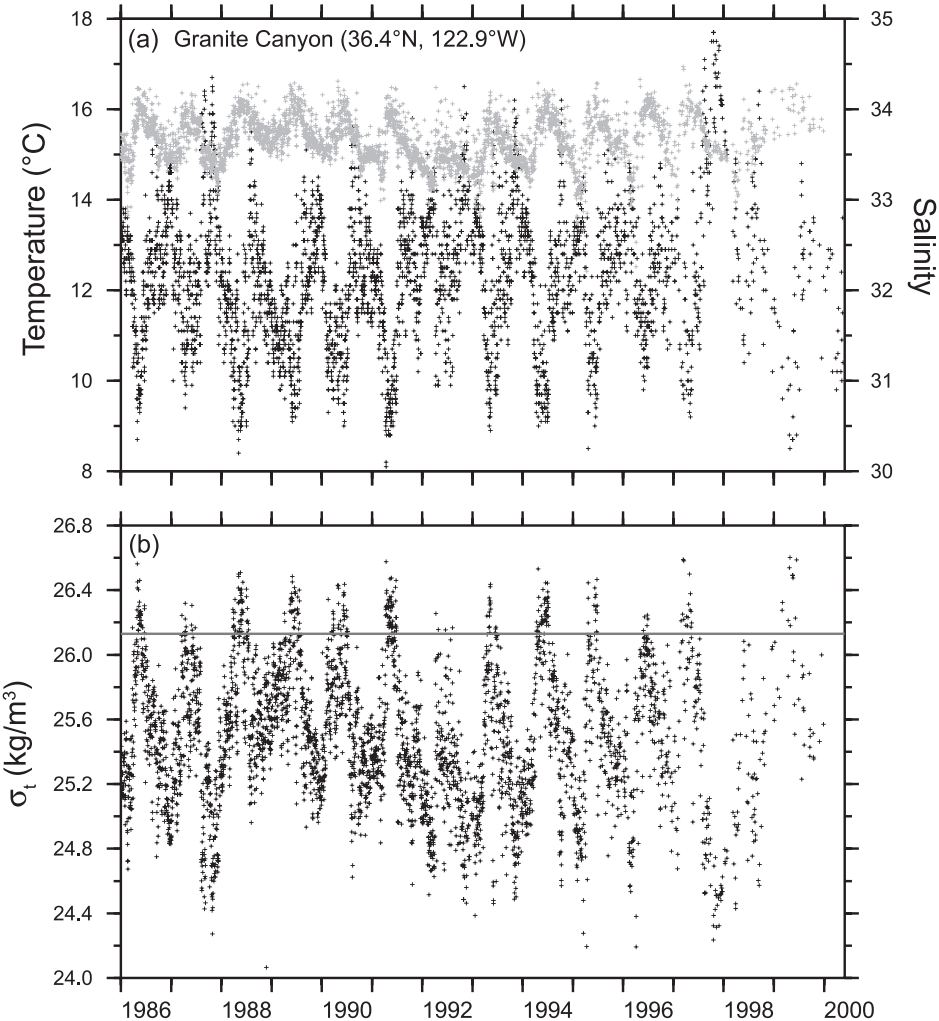

Figure 9. Time series of (a) surface temperature (black plusses) and surface salinity (gray plusses) and (b) corresponding surface density at Granite Canyon, California (36°25.9'N, 121°55'W), for the period January 1986 to May 2000. The gray line in (b) marks the density representing two standard deviations below the mean density of all identified inversion events (σ_θ = 26.13). The location of Granite Canyon is marked on the Figure 1 inset.

during the upwelling season at upstream coastal locations. For this we use the Granite Canyon shore station because it is has a relatively long time series of daily surface temperature and salinity measurements, and it represents the dominant coastal upwelling domain of the central California coast.

There is both a clear seasonal cycle and strong interannual variability in the temperature and salinity of surface waters at Granite Canyon (Fig. 9). Strong and persistent coastal upwelling in spring–summer (peaking in May) brings cool and salty (dense) waters to the

surface each year. Waters with temperatures less than 9°C and, especially, salinities greater than 34.00 psu are common in most summers (Fig. 9a). This results in at least a few observations each year of waters with surface densities greater than $\sigma_\theta = 26.2$, and greater than $\sigma_\theta = 26.4$ in most years (Fig. 9b). Over the 15-year record presented here, 3.2% (6.1%) of the daily observations at Granite Canyon had surface densities greater than $\sigma_t = 26.13$ ($\sigma_t = 26.25$), which corresponds closely with the percent of total station occupations with observed subduction signatures (Fig. 8). These waters are most likely high in inorganic nutrients as well; a CalCOFI cruise that sampled just offshore of Granite Canyon in April–May 1984 (stations 70.51 and 70.53) had 10 m nitrate levels over 26 μMol L^{-1} (Scripps Institution of Oceanography, 1984). We note that there are numerous data gaps in this time series, and also that near-surface waters farther north along the coast may be cooler and denser than those found at Granite Canyon. Clearly, waters with T-S characteristics similar to those observed for the CalCOFI deep oxygen inversions and subduction signatures are regularly brought up to or near the surface during seasonal coastal upwelling.

Superimposed on the annual cycle at Granite Canyon was significant interannual variability in both surface temperature and salinity. The El Niño events of 1987, 1992–93, and 1997–98 are clearly evident as years with anomalously high surface temperatures (up to 17.7°C in October 1997; Fig. 9a) and correspondingly lower maximum surface densities (Fig. 9b). The number of subduction signatures by season and year roughly matches this variability in upstream surface densities (Table 3). During the warm, El Niño-influenced periods in the early 1990s, 1997–98, and 2001–02, there were generally fewer subduction signatures detected (only 2 events each in 1994, 1997, 2001, and 2002). This does not mean that upwelling was weaker in these years, but that the source of the upwelled waters was warmer and, possibly, from a shallower level. The tight temperature-nitrate relationship for southern California Current waters (Kamikowski and Zentara, 1986) implies that these warmer upwelled waters also contained fewer nutrients, thus keeping production lower than other years (Bograd *et al*., 2001; Bograd and Lynn, 2001). However, the relationship between mean maximum surface density and number of observed subduction signatures is not strong, for obvious reasons: we neither know the source or age of the subduction signatures nor do we know how many features were missed with the limited CalCOFI sampling.

b. Subduction mechanisms

The following scenario could explain, in a general sense, the formation processes of the observed subducted water masses. Northerly to northwesterly winds that produce upwelling events along the central California coast are strongest during spring to early summer (Reid *et al*., 1958). Coastal surface water is transported offshore during this period and is replaced by water from below. Water from depths down to 200 meters rises to less than 50 meters at some coastal locations (Sverdrup, 1937); it need not rise completely to the surface to have its characteristics altered by photosynthetic processes. In fact, the relatively low mean saturation levels (less than 55%; Table 2) and high densities of the

Table 3. Temporal distribution of all identified subduction signatures in the CalCOFI record, 1984–2003. See Section 2c for event identification details. Seasons defined as in Table 1.

	Winter	Spring	Summer	Autumn	TOTAL
1984	7	5	1	3	16
1985	1	2	4	0	7
1986	1	1	0	2	4
1987	0	1	5	0	6
1988	0	0	3	1	4
1989	2	2	3	3	10
1990	0	0	2	2	4
1991	1	0	1	3	5
1992	0	1	1	1	3
1993	0	0	1	2	3
1994	1	0	0	1	2
1995	2	1	0	0	3
1996	4	3	0	1	8
1997	0	0	2	0	2
1998	0	1	3	0	4
1999	2	6	2	0	10
2000	2	0	3	0	5
2001	0	0	2	0	2
2002	0	0	1	1	2
2003	1	1	3	1	6
TOTAL	24	24	37	21	106

subduction signatures suggest that these water masses were not at the surface long enough to equilibrate with the atmosphere or be significantly warmed. While the dense water is within the euphotic zone, photosynthesis increases the dissolved oxygen concentration while reducing nutrient and dissolved carbon dioxide concentrations. Oxygen concentration may nearly double, yet remain below full saturation because the initial concentration of deep inshore waters is typically less than 2.5 mL L^{-1} (less than 40% saturation). If the biological changes take place below the surface, there would be little change in temperature or salinity of the water. Through subduction at fronts (see below), or following relaxation of upwelling, the inshore dense water then sinks to a neutral density level, but

with altered chemical characteristics. As upwelling occurs at several locations along the central and northern California coast, several features containing anomalous chemical characteristics may be present at the same time at various places in the CCS.

Because the photosynthetic layer is not very thick, the subsurface oxygen anomaly is also not very thick and could easily be missed with the usual cast sampling intervals. Thus, when these features are observed, they often appear as a single high oxygen value in an otherwise smooth profile. Examination of older CalCOFI data reports reveals that the oxygen value is occasionally not reported near the density level of $\sigma_\theta \sim 26.4$, suggesting that a secondary oxygen maximum may have been observed but was thought to be erroneous and was rejected. Since nutrient data were not generally taken in the early years, additional measurements could not be used to check for the presence of a subduction signature.

What is the specific mechanism by which upwelled waters might be subducted? There is evidence from the Coastal Transition Zone (CTZ) and earlier experiments off the northern California coast that subduction of water masses occurs within cold upwelling filaments (Kadko *et al*., 1991; Washburn *et al*., 1991; Flament *et al*., 1985), which are common features in sea surface temperature and ocean color satellite images of the CCS. From intensive hydrographic sampling of a cold filament observed off Pt. Arena (38N) in summer 1988, Kadko *et al*. (1991) found deficiencies of ^{222}Rn with respect to ^{226}Ra and dissolved oxygen maxima associated with layers of elevated chlorophyll-*a* below the euphotic zone. They concluded that the subsurface chlorophyll maxima were derived from the subduction of surface waters, and not produced by *in situ* phytoplankton growth or by particle settling. The ^{222}Rn deficiency suggested that the subducted water mass had recently been at the surface, and estimated the vertical transport at $\sim$25 m d^{-1}. Washburn *et al*. (1991) used profiles of fluorescence and beam attenuation coefficient to identify subducted water masses on all six grid surveys of the CTZ experiment, at densities ranging between $\sigma_\theta = 25.9$–26.6. This range encompasses most of the range of our observed deep oxygen inversions and subduction signatures (Figs. 5 and 6), although we limited our search to depths greater than $\sigma_\theta = 26.13$. The filament studies identified several processes that contributed to the subduction of water, most notably strong convergence at the axis of the offshore-flowing jet and flow along sloping isopycnal surfaces due to advection and mixing processes (Kadko *et al*., 1991; Washburn *et al*., 1991; Flament *et al*., 1985).

Using high-resolution hydrographic and bio-optical measurements in June-July 1993, Barth *et al*. (2002) observed high concentrations of chlorophyll at depths of 150–250 m (near $\sigma_\theta = 26.4$) and more than 300 km offshore of northern California, well below the depth to which light penetrates and far from the productive coastal upwelling region. They concluded that this feature was formed at the coast near Cape Mendocino and was transported offshore within the meandering California Current jet, traveling a distance of over 400 km in 25 days. Subduction occurred as the water mass was forced downward along sloping density surfaces through the conservation of potential vorticity along the meandering jet path. They estimated an export of approximately 2.4×10^6 kg of carbon out of the coastal zone within this single feature. Huyer *et al*. (2005) also report

observations of deep chlorophyll pockets within the main core of the coastal jet off Crescent City, California, in the summers of 2002 and 2003, and attribute these features to subduction of surface waters. These observations are entirely consistent with the subduction signatures observed in the CalCOFI region, and likely captured the typical formation process.

Subduction within coastal filaments is a likely source for the anomalous water masses seen in the CalCOFI record. But these water masses have undergone an unknown history from their time of formation, presumably near the coast, to their observation embedded at depths greater than 200 m within the main California Current flow. How are these subducted water masses transported to the CalCOFI region? The feature observed in August 1985 (Figs. 2–4) was contained within an eddy of diameter >80 km that was embedded within the main core of the California Current. We cannot fully resolve the dimensions of this eddy with the coarse spacing and nonsynoptic sampling (stations 80.80 and 77.80 were sampled 48 hours apart). Several other subduction signatures appeared to be associated with mesoscale eddies and were observed at more than one station on a single cruise. Unfortunately the spatial resolution of the sampling grid is not eddy-resolving, and the majority of subduction signatures were identified at single, isolated profiles. Simpson and Lynn (1990) have described subsurface anticyclonic eddies in the CalCOFI domain, of apparent California Undercurrent origin, that are characterized by a low oxygen and high spiciness core. The features described here, however, are characterized by an oxygen excess, hence an apparent oxygen *gain*. It is possible that Undercurrent waters provide a source for water masses that are upwelled and eventually subducted and observed downstream, but these waters would have undergone significant chemical alteration near the surface. With limited observations, it is clear that modeling efforts are needed to resolve the sources and mechanisms by which upwelled waters are subducted and transported within the California Current.

c. Subduction implications

Subduction signatures (and deep oxygen inversions) were observed in each season and in every year of the data set, suggesting that the processes that form these water masses are common and persistent. This is not surprising given the ubiquity of upwelling filaments seen in satellite images of the CCS, assuming these filaments provide a likely formation mechanism. But we note that the search criteria applied here are conservative, and that there are likely many other candidate subduction signatures in the record having a weaker signal, perhaps because the water masses were of greater age when observed. (We have classified only 17% of the observed deep oxygen inversions as true subduction signatures here.) Features at levels shallower than the $\sigma_\theta = 26.13$ isopycnal would also be missed. Additionally, the relatively coarse resolution of most of the CalCOFI grid is likely to miss smaller features, while the quarterly temporal resolution will miss short-lived features or those that transgress the grid between surveys. Given these limitations, the results presented here make clear that the subduction and subsequent advection of recently upwelled coastal waters is a common phenomenon in the CCS.

Persistent subduction of coastal waters implies a significant vertical transport of heat, mass, salt, and other scalars out of the surface layer, along with biogenic matter. The CTZ observations showed a vertical and offshore transport of a significant phytoplankton biomass, implying a high vertical flux of organic carbon out of the surface layer (Washburn *et al*., 1991). Observations from the Canary Current region have also shown a significant offshore export of nutrients and organic matter by coastal filaments and eddies, resulting in the enrichment of offshore oligotrophic waters throughout the year (Garcia-Munoz *et al*., 2005; Pelegri *et al*., 2005). Depending on the longevity of the biological signal, these water masses could provide an important prey source for opportunistic predators below the euphotic layer and well outside of the narrow coastal zone. If these subduction processes are occurring year-round over large portions of the coastal margin, this could represent an important sink of atmospheric CO_2 into the thermocline (Walsh *et al*., 1981; Liu *et al*., 2000; Barth *et al*., 2002; Hales *et al*., 2005).

The subduction and spreading of these oxygenated waters also provides a means to persistently ventilate the upper thermocline of the California Current. Ventilation of thermocline waters is generally believed to occur primarily at high latitudes during surface water mass formation (Sverdrup *et al*., 1942). The subduction processes described here provide an alternative mechanism to ventilate the thermocline within eastern boundary current systems, without significant alteration of water mass physical characteristics.

5. Summary and conclusions

We used 20 years of hydrographic data from the CalCOFI program off southern California to search for water mass signatures of subducted upwelled waters. A search for secondary oxygen maxima in more than 6000 water column profiles identified 629 cases of deep oxygen inversions. The additional criteria of a minimum magnitude of the deep oxygen inversion and an accompanying reduction in dissolved nutrients identified 106 (17%) of these as subduction signatures. The physical and chemical characteristics of these water masses suggest that they had been photosynthetically modified in the euphotic zone, and perhaps ventilated at the surface, before being subducted and eventually advected downstream within the California Current. Surface waters with similar physical characteristics as the deep oxygen inversions and subduction signatures ($\theta \sim 8.5°C$, $S \sim 34.0$ psu, $\sigma_\theta \sim 26.4$ kg m^{-3}) were observed during the spring–summer upwelling period at a shore station upstream from the CalCOFI grid. Even with conservative search criteria and coarse spatial-temporal sampling, these subduction signatures were observed in all seasons and in each year of the record. These results imply that the processes leading to the subduction, cross-shore transport, and downstream advection of upwelled water masses are common and persistent in the California Current System, and probably in other eastern boundary current systems as well. This has important implications for the transport of coastal waters, and resident planktonic organisms and organic carbon, out of the coastal euphotic zone, and provides a mechanism for frequent ventilation of the upper thermocline of eastern boundary current systems.

There are still a number of unresolved issues regarding the formation and evolution of

these subducted water masses. Since we do not know the sources of the subduction signatures observed in the CalCOFI grid, we cannot determine their ages, history, or ultimate fate. However, more than 40% of these events were observed out of the upwelling season, between October and March. This suggests that these water masses may be very long-lived (several weeks to months), or that their formation processes persist year-round. It is also unclear whether interannual variability in the timing, strength, and persistence of coastal upwelling (Schwing and Mendelssohn, 1997), or in the ambient properties of the upwelled waters, may impact the frequency and magnitude of subduction signatures.

Since most of these features were found at depths greater than the deepest chlorophyll-*a* samples, we cannot describe their biological characteristics. Additionally, water masses of ages greater than a few weeks, as these may be, may have lost any biological signal. Future work will look at the oxygen record from the 1950–84 CalCOFI data set; although very little corroborating nutrient data are available for this time period, a census of secondary oxygen maxima can be made. The longer time series of identified deep oxygen inversions may elucidate more clearly the impact of interannual to decadal forcing (e.g., El Niño events and large-scale regime shifts) on their frequency of formation. However, high-resolution modeling studies are needed to elucidate the subduction mechanisms and to clarify the evolution and biophysical significance of these subducted water masses.

Acknowledgments. We thank Xuemei Qiu for analysis and graphics assistance. We acknowledge the quality and longevity of the CalCOFI program, and the many scientists and seagoing staff who have contributed to the collection, processing, and analysis of this excellent data set. We also acknowledge the California Current Ecosystem Long-Term Ecosystem Research (CCE-LTER) project, supported by a grant from NSF (OCE-0417616). We thank Roberta Hamme, Daniel Palacios, Elizabeth Venrick, and two anonymous reviewers for helpful comments on earlier drafts.

REFERENCES

Anderson, G. C. 1971. Oxygen analysis, *in* Marine Technician's Handbook, SIO Ref. 71-8, Scripps Inst. of Oceanography, La Jolla, CA.

Atlas, E. L., J. C. Callaway, R. D. Tomlinson, L. I. Gordon, L. Barstow and P. K. Park. 1971. A practical manual for use of the Technicon AutoAnalyzer in seawater nutrient analysis. Oreg. State Univ. Tech. Rep. 215, Corvallis, OR.

Barth, J. A., T. J. Cowles, P. M. Kosro, R. K. Shearman, A. Huyer and R. L. Smith. 2002. Injection of carbon from the shelf to offshore beneath the euphotic zone in the California Current. J. Geophys. Res., *107,* doi:10.1029/2001JC000956.

Bograd, S. J., T. K. Chereskin and D. Roemmich. 2001. Transport of mass, heat, salt, and nutrients in the southern California Current System: Annual cycle and interannual variability. J. Geophys. Res., *106,* 9255–9275.

Bograd, S. J. and R. J. Lynn. 2001. Physical-biological coupling in the California Current during the 1997–99 El Niño-La Niña cycle. Geophys. Res. Lett., *28,* 275–278.

Carpenter, J. H. 1965. The Chesapeake Bay Institute technique for the Winkler dissolved oxygen method. Limnol. Oceanogr., *10,* 141–143.

Chereskin, T. K., M. Y. Morris, P. P. Niiler, P. M. Kosro, R. L. Smith, S. R. Ramp, C. A. Collins and D. L. Musgrave. 2000. Spatial and temporal characteristics of the mesoscale circulation of the California Current from eddy-resolving moored and shipboard measurements. J. Geophys. Res., *105,* 1245–1270.

Flament, P., L. Armi and L. Washburn. 1985. The evolving structure of an upwelling filament. J. Geophys. Res., *90,* 11,765–11,778.

Garcia, H. and L. Gordon. 1992. Oxygen solubility in seawater: Better fitting equations. Limnol. Oceanogr., *37,* 1307–1312.

Garcia-Munoz, M., J. Aristegui, J. L. Pelegri, A. Antoranz, A. Ojeda and M. Torres. 2005. Exchange of carbon by an upwelling filament off Cape Ghir (NW Africa). J. Mar. Syst., *54,* 83–95.

Gordon, L. I., J. C. Jennings, A. A. Ross and J. M. Krest. 1993. A suggested protocol for continuous flow automated analysis of seawater nutrients (phosphate, nitrate, nitrite and silicic acid) in the WOCE Hydrographic Program and the Joint Global Ocean Flux Study, WOCE Operations Manual, Part 3.1.3, WHP Office Report WHPO 91-1.

Hales, B., T. Takahashi and L. Bandstra. 2005. Atmospheric CO_2 uptake by a coastal upwelling system. Global Biogeochem. Cycles, *19,* doi:10.1029/2004GB002295.

Hayward, T. L. 1994. The shallow oxygen maximum layer and primary production. Deep-Sea Res., Part I, *41,* 559–574.

Hickey, B. A. 1979. The California Current system: Hypotheses and facts. Prog. Oceanogr., *8,* 191–279.

Huyer, A., J. H. Fleischbein, J. Keister, P. M. Kosro, N. Perlin, R. L. Smith and P. A. Wheeler. 2005. Two coastal upwelling domains in the northern California Current System. J. Mar. Res., *63,* 901–929.

Kadko, D. C., L. Washburn and B. Jones. 1991. Evidence of subduction within cold filaments of the northern California coastal transition zone. J. Geophys, Res., *96,* 14,909–14,926.

Kamikowski, D. and S.-J. Zentara. 1986. Predicting plant nutrient concentration from temperature and sigma-*t* in the world ocean. Deep-Sea Res., Part I, *33,* 89–105.

Liu, K. K., K. Iseki and S. Y. Chao. 2000. Continental margin carbon fluxes, *in* The Changing Carbon Cycle, R. B. Hanson, H. W. Ducklow and J. G. Field, eds., Cambridge University Press, NY, 187–239.

Lynn, R. J., S. J. Bograd, T. K. Chereskin and A. Huyer. 2003. Seasonal renewal of the California Current: The spring transition off California. J. Geophys. Res., *108,* doi:10.1029/2003JC001787.

Lynn, R. J. and J. J. Simpson. 1987. The California Current System: the seasonal variability of its physical characteristics. J. Geophys. Res., *92,* 12,947–12,966.

Pelegri, J. L., J. Aristegui, L. Cana, M. Gonzalez-Davila, A. Hernandez-Guerra, S. Hernandez- Leon, A. Marrero-Diaz, M. F. Montero, P. Sangra and M. Santana-Casiano. 2005. Coupling between the open ocean and the coastal upwelling region off northwest Africa: water recirculation and offshore pumping of organic matter. J. Mar. Sys., *54,* 3–37.

Reid, J. L., Jr. 1962. Distribution of dissolved oxygen in the summer thermocline. J. Mar. Res., *20,* 138–148.

Reid, J. L., Jr., G. I. Rode and J.G. Wyllie. 1958. Studies of the California Current System. CalCOFI Rep., *1,* 27–57.

Schwing, F. B. and R. Mendelssohn. 1997. Increased coastal upwelling in the California Current System. J. Geophys. Res., *102,* 3421–3438.

Scripps Institution of Oceanography. 1984. Physical, chemical, and biological data, CalCOFI cruises 8404, 8405, and 8406, SIO Ref. 84-25, La Jolla, CA, 224 pp.

Scripps Institution of Oceanography. 1986. Physical, chemical, and biological data, CalCOFI cruises 8508 and 8511, SIO Ref. 86-6, La Jolla , CA, 96 pp.

Scripps Institution of Oceanography. 1991. Physical, chemical, and biological data, CalCOFI cruises 9003 and 9004, SIO Ref. 91-4, La Jolla, CA, 96 pp.

Scripps Institution of Oceanography. 2002. Physical, chemical, and biological data, CalCOFI cruises 0101 and 0104, SIO Ref. 02-07, La Jolla CA, 104 pp.

Simpson, J. J. and R. J. Lynn. 1990. A mesoscale eddy dipole in the offshore California Current. J. Geophys. Res., 95, 13,009–13,022.

Stefansson, U. and F. A. Richards. 1964. Distributions of dissolved oxygen, density and nutrients off the Washington and Oregon coasts. Deep-Sea Res., Part I, *11,* 355–380.

Strub, P. T. and C. James. 2000. Altimeter-derived variability of surface velocities in the California Current System: 2. Seasonal circulation and eddy statistics. Deep-Sea Res., Part II, *47,* 831–870.

Sverdrup, H. U. 1937. On the process of upwelling, J. Mar. Res., *1,* 155–164.

Sverdrup, H. U., M. W. Johnson and R. H. Fleming. 1942. The Oceans, Their Physics, Chemistry, and General Biology, Prentice-Hall, Englewood Cliffs, NJ, 1087 pp.

Walsh, J. J., G. T. Rowe, R. L. Iverson and C. P. McRoy. 1981. Biological export of shelf carbon is a sink of the global CO_2 cycle. Nature, *291,* 196–201.

Washburn, L., D. C. Kadko, B. H. Jones, T. Hayward, P. M. Kosro, T. P. Stanton, S. Ramp and T. Cowles. 1991. Water mass subduction and the transport of phytoplankton in a coastal upwelling system. J. Geophys. Res., *96,* 14,927–14,945.

Wooster, W. S. and J. L. Reid, Jr. 1963. Eastern boundary currents, *in* The Sea, M.N. Hill, ed., Wiley Interscience, NY, 253–280.

Received: *15 February, 2005*; revised: *20 April, 2005*.